Contents lists available at ScienceDirect

Neuropsychologia

journal homepage: www.elsevier.com/locate/neuropsychologia

Disentangling representations of shape and action components in the tool network

Xiaoying Wang[a,b,1], Tonghe Zhuang[a,b,1], Jiasi Shen[a,b], Yanchao Bi[a,b,*]

[a] State Key Laboratory of Cognitive Neuroscience and Learning & IDG/McGovern Institute for Brian Research, Beijing Normal University, Beijing 100875, China
[b] Beijing Key Laboratory of Brain Imaging and Connectomics, Beijing Normal University, Beijing 100875, China

ARTICLE INFO

Keywords:
Object representation
Tool network
Shape
Action
Pattern analysis
fMRI

ABSTRACT

Shape and how they should be used are two key components of our knowledge about tools. Viewing tools preferentially activated a frontoparietal and occipitotemporal network, with dorsal regions implicated in computation of tool-related actions and ventral areas in shape representation. As shape and manners of manipulation are highly correlated for daily tools, whether they are independently represented in di□erent regions remains inconclusive. In the current study, we collected fMRI data when participants viewed blocks of pictures of four

cortex and LOTC within which tool-selective activations were frequently observed and their underlying white-matter pathways, were also frequently shown to be involved in action recognition and production as well as action (manipulation) knowledge retrieval (Buxbaum et al., 2000, 2007; Buxbaum and Sa□ran, 2002; Tranel et al., 2003; Lewis, 2006; Negri et al., 2007; Kalénine et al., 2010; Bi et al., 2015; Tarhan et al., 2015; Lingnau and Downing, 2015; Chen et al., 2016, 2017b; Buxbaum, 2017). Even the occipitotemporal regions which were classically assumed to represent object shapes (James et al., 2003; Haushofer et al., 2008; Karnath et al., 2009; Peelen and Caramazza, 2012; Peelen et al., 2014) could di□erentiate between tools with different manners of manipulation (Chen et al., 2016, in and around extrastriate body area), make predictions of upcoming motor actions through activation patterns (Gallivan et al., 2013), and exhibit motor-related repetition suppression e□ect (Mahon et al., 2007).

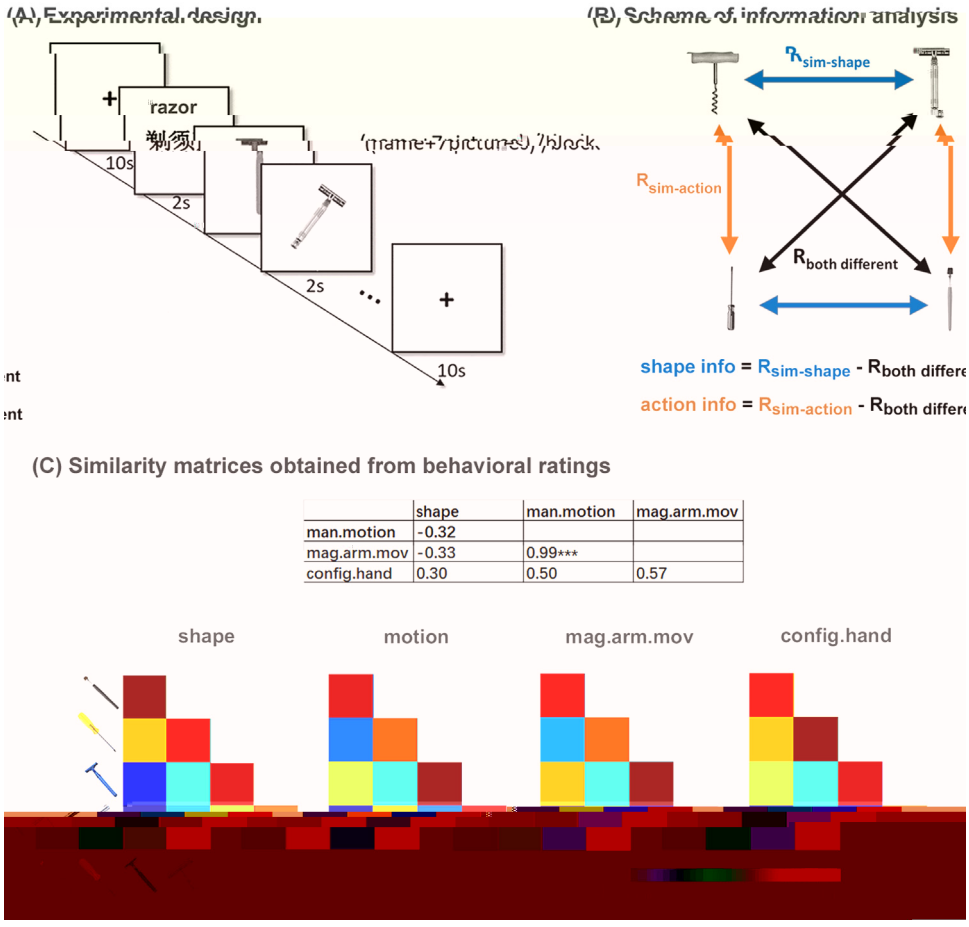

	shape	man.motion	mag.arm.mov
man.motion	-0.32		
mag.arm.mov	-0.33	0.99***	
config.hand	0.30	0.50	0.57

Fig. 1. (A) Design of the fMRI experiment; (B) Scheme of information analysis and (C) Similarity matrices of shape and di□erent action components obtained from behavioral ratings by an independent participant group (N = 20) and the matrix of correlations between shape and action components. The color bar indicates the degree of similarity. Asterisks indicate significant correlation.

stimuli pictures indicated the similarity between them. For shape similarity judgment, participants were asked to arrange the stimuli pictures according to the perceived overall shape similarity of the objects, with examples denoting similar (orange - ball) and dissimilar (wolf - snake) pairs given as references. For manner of motion, participants were asked to arrange the pictures based on the similarity of the moving trajectories when using di□erent objects, and the similar and dissimilar example pairs given were “key - light bulb” and “saw - key”, respectively; For magnitude of arm movement, participants were asked to arrange the pictures according to how similar amount the arm moved when using the objects, and the similar and dissimilar example pairs given were “ax-saw” and “ax-pen”;For configuration of hand, participants were asked to arrange the pictures based on the similarity of the hand posture, along with the similar example pair of “ax - shovel” and dissimilar example pair “ax - pen” given as references. The arrangements terminated when available time (i.e., 1 h) was up or the dissimilarity-evidence criterion (i.e., 0.5) was reached (Kriegeskorte and Mur, 2012). On average, it took about 30–40 min for each rating to stop for our participants. For each participant, a mean similarity score was obtained for each object pair by averaging similarity scores across all corresponding pairs of exemplars.

During the main fMRI experiment (Fig. 1A), participants viewed blocks of the four objects, with each block started with one object name and followed by 7 pictures of object exemplars. Participants were asked to judge whether all exemplars in the block was consistent with the object name by pressing corresponding buttons (all consistent, right index finger; otherwise, right middle finger). Participants were instructed to respond right after the disappearance of the last picture of each block as correctly and quickly as possible. Inconsistent blocks were assigned to one regressor of no interest (the “oddball” condition) when building general linear model (GLM) and were not included into subsequent analyses. Thus, all object conditions were supposed to be associated with identical button-press responses (i.e., right index finger press), ruling out the potential confounding of di□erent motor responses.

Six runs were scanned for each participant. Each run lasted for 270 s, began and ended with a 10 s fixation period, during which a fixation cross was presented at the center of the screen. Each run was consisted of 10 task blocks (16 s each) separated by 10 s fixation periods. The 10 task blocks included two blocks per object and two oddball blocks within which inconsistent exemplars were presented. Each visual stimuli (i.e., object names and pictures) was presented for 2 s. The object exemplars presented in each block varied in four orientations (i.e., horizontal, vertical, 45°, 135°) to avoid visual adaptation. The orientation of object exemplars was balanced across di□erent blocks. The block order was counterbalanced across runs.

A single-run tool localizer experiment was conducted to localize tool-selective regions. Participants viewed blocks of pictures of tools and large manmade objects and pressed a button with their right index finger as soon as possible when they detected a picture appeared twice in a row. Thirty pictures of di□erent items were selected for each category for stimuli. The whole run lasted for 426 s in total, was consisted of 16 blocks, with 8 blocks per category. Fixation cross periods (10 s) were presented at the beginning and at the end of the whole run, as well

as between blocks. Each block was consisted of 16 pictures (200 ms presentation, 800 ms fixation). The order of pictures was randomized across blocks and the presentation order of blocks was counterbalanced between categories. There were 0–2 catch trials per block. The number of button presses was matched between the two categories (8 times per category in total).

2.3. Image acquisition and preprocessing

All functional and structural MRI data were collected on a 3 T Siemens Trio Tim Scanner at the Beijing Normal University MRI center. For structural MRI, high-resolution anatomical three-dimensional magnetization-prepared rapid gradient echo (3D-MPRAGE) images were collected in the sagittal plane: 144 slices, repetition time (TR) = 2530 ms, echo time (TE) = 3.39 ms, Flip Angle (FA) = 7°, Matrix Size = 256 × 256, Voxel Size = 1.33 × 1 × 1.33 mm^3. BOLD fMRI data was collected using an echo-planar imaging (EPI) sequence that covered the whole cerebral cortex and the cerebellum: 33 axial slices, TR = 2000 ms, TE = 30 ms, FA = 90°, matrix size = 64 × 64, voxel size = 3 × 3 × 3.5 mm^3 with gap of 0.7 mm).

Data were preprocessed using Statistical Parametric Mapping software (SPM12; http://www.fil.ion.ucl.ac.uk/spm/software/spm12/). Preprocessing procedure included slice timing, head motion correction, low-frequency drifts removal with a temporal high-pass filter (cut-off: 0.008 Hz), and normalization into the Montreal Neurological Institute (MNI) space using unified segmentation. The functional images were resampled to 3 mm isotropic voxels and the data of the tool localizer experiment were further spatially smoothed using a 6 mm FWHM Gaussian kernel.

2.4. Data analysis

Functional data were analyzed using the general linear model (GLM) in SPM12. For the main experiment, the GLM included the 4 predictors corresponding to the 4 objects respectively, one predictor of [illegible]

2.4.3. Whole–brain analyses

Whole-brain information searchlight analyses were conducted to find additional regions carrying significant shape or action information. Shape and action information were computed similarly as above for each search sphere (10 mm radius) centered on each voxel in the whole brain. The information values were then assigned to the center voxel and corresponding information maps were thus generated for each participant. A random-e□ects group analysis was performed on the spatially smoothed (FWHM = 6) information maps using the permutation-based statistical nonparametric mapping (SnPM; http://go.warwick.ac.uk/tenichols/snpm) to test for significant shape or action information. The significance threshold was defined as cluster-level corrected FWE $p < 0.05$ (voxel $p < 0.01$, variance smoothing = 0, permutation = 5000) for all analyses.

RSA searchlight analyses were also conducted to identify regions carrying representations of object shapes and di□erent components of object-directed actions in the whole brain. For each search sphere (10 mm radius), the multi-voxel activation patterns were extracted for the four objects and correlated with each other to obtain a neural RSM. Correlations were computed between neural RSM and behavioral RSMs and the resulting r values then assigned to the center voxel, resulting corresponding r maps for each participant. The r maps were then Fisher-transformed and spatially smoothed (FWHM = 6) and entered to random-e□ects group analyses using SnPM. Similar threshold was used as in the information searchlight analyses.

All results in this paper are shown in the MNI space and projected onto the MNI brain surface using the BrainNet viewer (http://www.nitrc.org/projects/bnv/) (Xia et al., 2013).

3. Results

3.1. Behavioral results

In the main experiment, participants viewed blocks of pictures of corkscrew, paintbrush, razor and screwdriver and were asked to judge whether all pictures in each block were consistent with the cue word presented at the beginning of the block by pressing buttons. No significant di□erence was observed between the four object conditions on either response times (mean ± SE: paintbrush = 815 ± 123 ms, screwdriver = 736 ± 62 ms, corkscrew = 736 ± 61 ms, razor = 729 ± 75 ms; $F_{(3,87)} = 0.456$, $p = 0.716$) or accuracies (mean ± SE: paintbrush = 98.1% ± 13.6%, screwdriver = 98.0% ± 13.6%, corkscrew = 93.9% ± 23.9%, razor = 97.7% ± 1theed4cthe

Table 1
Group-defined tool-selective ROIs ($p < 0.05$, FWE corrected).

Area	Coordinates			Peak t value (df = 21)	No. of voxels	Brodmann Regions
	x	y	z			
left SPL/IPL	− 27	− 48	54	8.82	738	1/2/3/4/5/7/22/40
left LOTC	− 51	− 66	6	8.00	319	18/19/21/22/37/39
left Prec/PM	− 24	− 9	57	6.49	124	6
left MFG/IFG	− 45	36	18	5.32	40	10/46
right LOTC	54	− 66	0	8.07	180	19/21/37/39
right SMG	60	− 33	27	5.61	73	40
right SPL/IPL	27	− 42	45	4.98	190	1/2/3/7

3.2. Shape and action representations in tool-selective ROIs

The whole-brain random-effects group analysis of the contrast of tool > large manmade objects (voxel $p < 0.001$, cluster size ≥ 40, FWE corrected $p < 0.05$ at cluster level) yielded the classical tool network: the bilateral LOTC encompassing the middle temporal gyrus and inferior and middle occipital gyrus, the bilateral superior/inferior parietal lobe (SPL/IPL) including the left supramarginal gyrus (SMG), the right SMG, the left precentral/premotor cortex (Prec/PM) and the left middle and inferior frontal gyrus (MFG/IFG) (Fig. 2A & Table 1).

To test for the object shape and action representations in these tool-selective ROIs, we first computed shape and action information for each ROI by subtracting the average of correlations between activation patterns to tools different in both dimensions from the average of correlations between activation patterns to tools similar in one dimension but different in the other (see Fig. 1 and Method). As presented in Fig. 2A and Table 2, one-tailed one-sample *t*-tests identified significant *shape* information in the bilateral LOTC, the bilateral SPL/IPL and the left Prec/PM cortex ($t_{(20)} > 2.24$. Bonferroni corrected $p < 0.05$). Significant *action* information was observed in the left Prec/PM cortex and bilateral SPL/IPL ($t_{(20)} > 2.17$, Bonferroni corrected $p < 0.05$) and in the left MFG/IFG at an uncorrected level ($t_{(20)} = 1.85$, uncorrected $p = 0.039$). No significant effect of either dimension was observed in the right SMG ($t_{(20)} < 1.20$, uncorrected $p > 0.122$, see Table 2 for detailed information). Directly comparing the magnitude of the two types of information using two-tailed paired *t*-tests, we found that shape information was significantly richer than action information in the bilateral LOTC (left: $t_{(20)} = 3.62$, $p < 0.002$; right: $t_{(20)} = 4.45$, $p < 0.001$). No significant difference between shape and action information was observed in other ROIs (ps > 0.13, Table 2). The patterns of results based on data without demeaning were largely similar (Supplementary Table 1).

We also conducted analyses in ROIs defined at individual subject level (see Method). As shown in Fig. 2B and Supplementary Table 2, we computed shape and action information in the individually defined ROIs which could be identified in at least 11 participants (> 50% participants), which were the bilateral LOTC and SPL/IPL ROIs. Similar as the results of the group-based ROI information analyses, the bilateral LOTC showed significant shape information (left: 0.33 ± 0.06, $t_{(19)} = 5.66$, $p < 0.001$; right: 0.23 ± 0.11, $t_{(12)} = 2.10$, $p < 0.029$) but insignificant action information (left: −0.002 ± 0.06, $t_{(19)} = 0.03$, $p = 0.510$; right: − 0.001 ± 0.08, $t_{(12)} = 0.01$, $p = 0.507$). The differences between shape and action information were significant in the bilateral individual-based LOTC ROIs as well (shape vs. action, left: $t_{(19)} = 4.10$, $p < 0.001$; right: $t_{(12)} = 2.38$, $p < 0.035$). The left SPL/IPL also exhibited similar pattern as in the results of group-based ROI analyses, containing both shape (0.23 ± 0.09, $t_{(15)} = 2.55$, $p < 0.011$) and action (0.24 ± 0.06, $t_{(15)} = 4.14$, $p < 0.001$) information in an indistinguishable manner (shape vs. action, $t_{(15)} = 0.07$, $p = 0.947$). While for the right SPL/IPL, the action information was still significant (0.36 ± 0.14, $t_{(10)} = 2.48$, $p < 0.016$) but the shape information become insignificant (0.14 ± 0.13, $t_{(10)} = 1.08$, $p = 0.152$). No significant difference was observed between shape and action information in the right IPL (shape vs. action, $t_{(10)} = -1.28$, $p = 0.230$). Frontal regions were not investigated due to low ROI identification rate across individual participants (< 7 participants). The patterns of results based on data without demeaning were largely similar (Supplementary Table 2).

We further carried out RSAs to test the effects of object shapes against potential finer action components (action kinematics and hand configurations) in the tool network using subjective measures. As shown in Table 3 and Fig. 3A, the neural RSMs of the bilateral LOTC and the left SPL/IPL ROIs were significantly correlated with the rating-derived object shape RSM ($t_{(20)} > 2.60$, Bonferroni corrected $p < 0.05$). After controlling for the effect of action kinematics and configuration of hand (Fig. 3B), the bilateral LOTC still showed significant shape representation ($t_{(20)} > 2.30$, Bonferroni corrected $p < 0.05$), while the shape effect in left SPL/IPL weakened ($t_{(20)} = 1.73$, uncorrected $p < 0.049$). Significant correlations with RSMs of action kinematics were identified in the left MFG/IFG and the left Prec/PM ROIs (Fig. 3A, $t_{(20)} > 2.72$, Bonferroni corrected $p < 0.05$). After controlling for the shape and configuration of hand (Fig. 3B), the action kinematics effect in the left MFG/IFG survived ($t_{(20)} = 2.49$, Bonferroni corrected $p < 0.05$) whereas those in the left Prec/PM ROI weakened ($t_{(20)} = 1.93$, uncorrected $p < 0.034$). The configuration of hand RSM correlated significantly with the neural RSMs of the bilateral LOTC, the left SPL/IPL and the left Prec/PM (Fig. 3A, $t_{(20)} > 2.82$, Bonferroni corrected $p < 0.05$). Weaker effects of hand configuration were also observed in the right SPL/IPL and SMG ROIs ($t_{(20)} > 1.88$, uncorrected $p < 0.05$). However, only the right LOTC remained to be correlated with the configuration of hand after controlling for object shape and action kinematics RSMs (Fig. 3B, $t_{(20)} = 2.32$, Bonferroni corrected $p < 0.05$). The patterns of results based on data without demeaning

Table 2
Shape and action information in group-defined tool-selective ROIs.

	Shape			Action			Shape vs. action	
	mean ± s.e.m	$t_{(20)}$	p	mean ± s.e.m	$t_{(20)}$	p	$t_{(20)}$	p
L LOTC	0.30 ± 0.05	6.45	< 0.001*	0.03 ± 0.06	0.60	0.278	4.19	< 0.001*
L SPL/IPL	0.17 ± 0.06	2.99	0.004*	0.12 ± 0.05	2.34	0.015*	0.71	0.484
L Prec/PM	0.13 ± 0.04	3.04	0.003*	0.19 ± 0.05	3.75	0.001*	− 0.81	0.426
L MFG/IFG	0.05 ± 0.12	0.41	0.343	0.18 ± 0.10	1.85	0.039	− 1.30	0.210
R LOTC	0.24 ± 0.07	3.32	0.002*	− 0.03 ± 0.05	− 0.59	0.719	3.85	< 0.001*
R SPL/IPL	0.13 ± 0.06	2.24	0.018*	0.15 ± 0.07	2.17	0.021*	− 0.17	0.863
R SMG	0.09 ± 0.08	1.09	0.144	0.11 ± 0.09	1.20	0.122	− 0.22	0.826

Note: P values shown in the table were uncorrected p values. Significant results after Bonferroni correction for multiple comparison (no. of corrections = 2) were denoted by asterisks.

Table 3
RSA results in group-defined tool-selective ROIs.

		r			Partial r (remove the other two variables)		
		mean ± s.e.m.	t	p	mean ± s.e.m.	t	p
shape	L LOTC	0.88 ± 0.12	7.41	< 0.001*	1.35 ± 0.20	6.77	< 0.001*
	L SPL/IPL	0.40 ± 0.15	2.60	0.008*	0.47 ± 0.27	1.73	0.049
	L Prec/PM	0.21 ± 0.16	1.32	0.100	0.35 ± 0.30	1.14	0.134
	L MFG/IFG	− 0.05 ± 0.19	− 0.27	0.604	0.05 ± 0.30	0.18	0.428
	R LOTC	0.78 ± 0.15	5.20	< 0.001*	0.73 ± 0.32	2.30	0.016*
	R SPL/IPL	0.25 ± 0.18	1.39	0.09	0.39 ± 0.24	1.62	0.060
	R SMG	0.25 ± 0.17	1.46	0.08	0.18 ± 0.30	0.61	0.275
action kinematics	L LOTC	− 0.13 ± 0.14	− 0.94	0.822	0.10 ± 0.32	0.30	0.385
	L SPL/IPL	0.23 ± 0.16	1.43	0.084	0.21 ± 0.24	0.89	0.193
	L Prec/PM	0.53 ± 0.16	3.41	0.001*	0.52 ± 0.27	1.93	0.034
	L MFG/IFG	0.49 ± 0.18	2.72	0.007*	0.63 ± 0.25	2.49	0.011*
	R LOTC	− 0.35 ± 0.13	− 2.61	0.992	− 0.36 ± 0.29	− 1.21	0.881
	R SPL/IPL	0.21 ± 0.19	1.07	0.149	0.34 ± 0.22	1.54	0.069
	R SMG	0.08 ± 0.17	0.51	0.309	− 0.02 ± 0.28	− 0.08	0.531
configuration of hand	L LOTC	0.35 ± 0.10	3.46	0.001*	0.08 ± 0.26	0.32	0.374
	L SPL/IPL	0.40 ± 0.11	3.65	0.001*	0.23 ± 0.21	1.10	0.142
	L Prec/PM	0.43 ± 0.09	4.74	< 0.001*	0.24 ± 0.24	0.99	0.167
	L MFG/IFG	0.10 ± 0.11	0.88	0.195	− 0.18 ± 0.21	− 0.84	0.795
	R LOTC	0.27 ± 0.09	2.82	0.005*	0.50 ± 0.21	2.32	0.016*
	R SPL/IPL	0.21 ± 0.11	1.88	0.038	− 0.02 ± 0.16	− 0.14	0.554
	R SMG	0.24 ± 0.12	1.96	0.032	0.22 ± 0.23	0.98	0.170

Note: p values shown in the table were uncorrected p values. Significant results after Bonferroni correction for multiple comparisons (no. of corrections = 3) were denoted by asterisks.

were largely similar (Supplementary Table 3).

3.3. Shape and action representations in the whole brain

Whole-brain information-based searchlight analyses were performed (Kriegeskorte et al., 2006) to uncover any additional brain

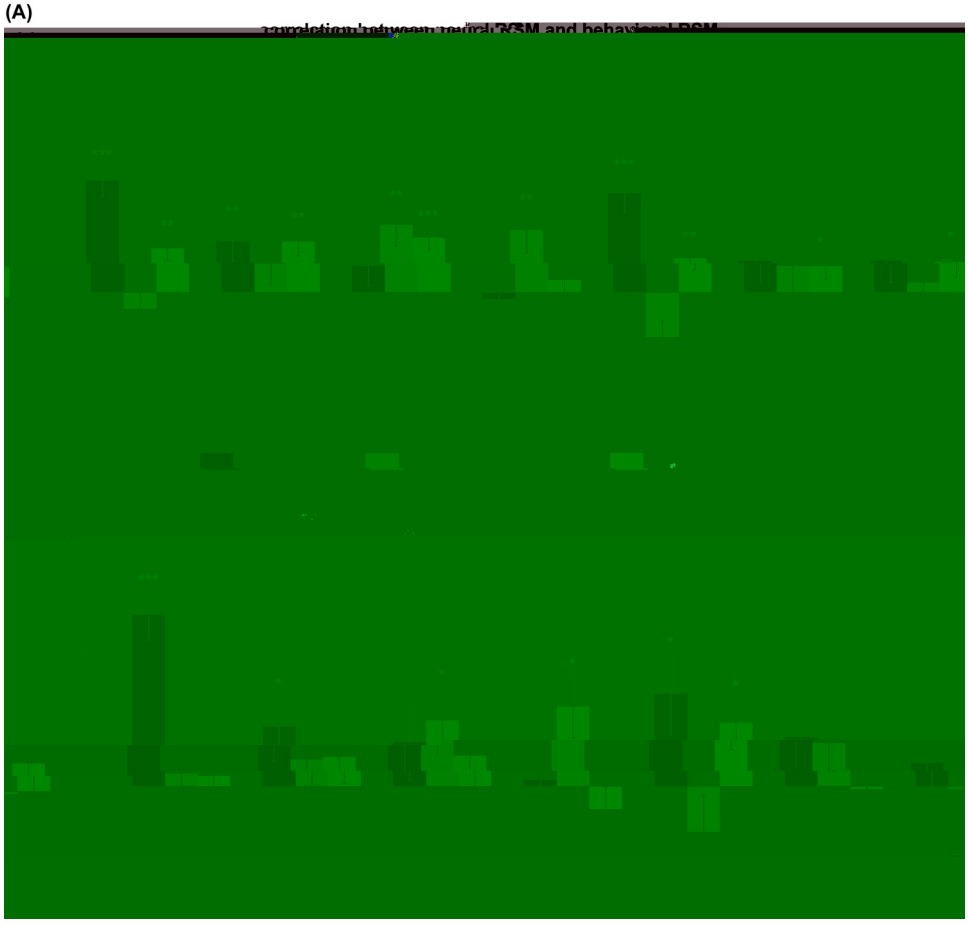

Fig. 3. RSA results based on the group-defined tool-selective ROIs. The bar plots show (A) correlations between neural RSMs and behaviorally derived RSMs on shape, motion/movement and configuration of hand; (B) partial correlations between neural RSMs and behaviorally derived shape, action kinematics and configuration of hand RSMs. For each behavioral RSM being tested, the two other models were controlled for to investigate the unique neural representation of the model being tested. Error bars in the bar plots indicate standard errors. Asterisks indicate the significance level before multiple comparison correction. ***, $p < 0.001$; **, $p < 0.01$, *, $p < 0.05$.

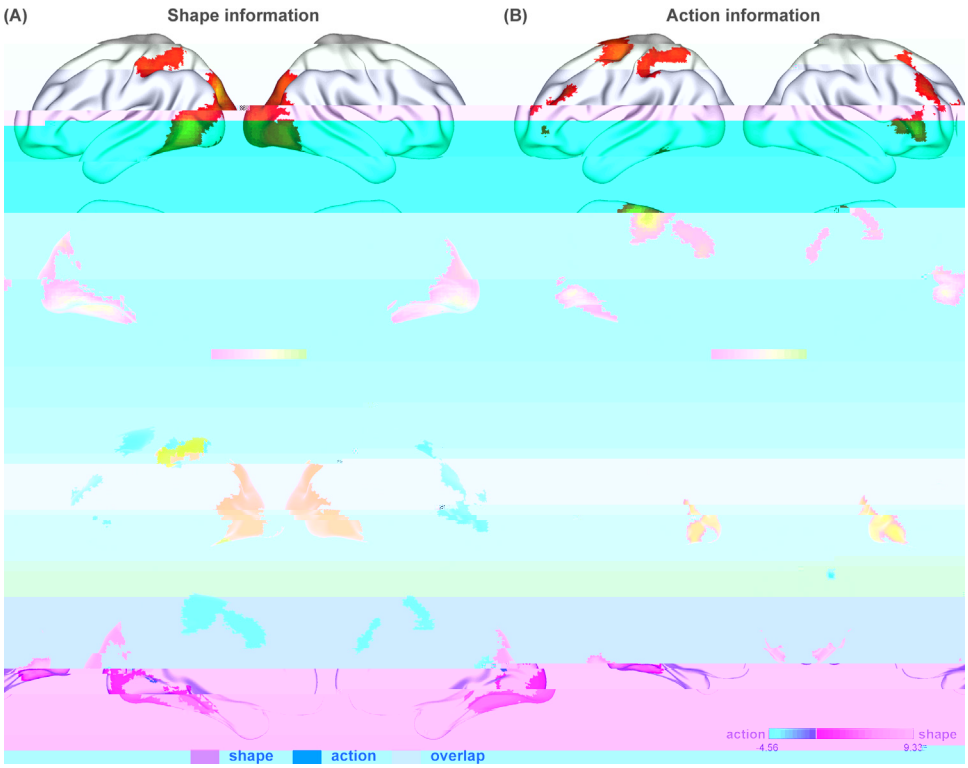

Fig. 4. Results of the whole-brain searchlight of (A) shape information and (B) action information; (C) the overlap (yellow) between shape (orange) and action (blue) information; and (D) the comparison between shape (warm-colored) and action (cold-colored) information. (A) and (B) were thresholded at FWE-corrected $p < 0.05$ at the cluster level, with the height threshold of $p < 0.01$; (D) was thresholded at uncorrected $p < 0.001$, cluster size > 10 voxels.

regions carry shape or action information. Significant shape information was observed in vast regions of the bilateral occipital cortex, inferior and middle temporal cortex and posterior inferior and superior parietal cortex (voxel $p < 0.01$, FWE corrected $p < 0.05$ at cluster level, Fig. 4A). Significant action information was observed in the bilateral supplementary motor area, precentral and premotor cortex, the right middle and inferior frontal cortex as well as the bilateral lingual gyrus (voxel $p < 0.01$, FWE corrected $p < 0.05$ at cluster level, Fig. 4B). As shown in Fig. 4C (yellow patches), significant information of both shape and action was observed in the left SPL/IPL (221 overlapping voxels) and the bilateral lingual gyrus (972 overlapping voxels). Comparison between the two types of information across the whole brain identified significantly stronger shape information in vast regions of bilateral occipitotemporal cortex (voxel $p < 0.001$, FWE corrected $p < 0.05$ at cluster level, warm colored clusters in Fig. 4D). Regions in the right middle frontal gyrus showed a trend of carrying more action information (uncorrected $p < 0.001$, cluster size > 10, cold colored clusters in Fig. 4D). Largely similar patterns were observed for results based on data without demeaning (Supplementary Fig. 1).

Whole-brain RSA searchlight analyses were also conducted to explore brain regions sensitive to finer aspects of tool-use actions. As shown in Fig. 5 (top left), the neural RSMs of vast regions of the bilateral occipital cortex, inferior and middle temporal cortex and a small portion of posterior SPL showed significant correlation with rating-derived shape RSM (voxel $p < 0.01$, FWE corrected $p < 0.05$ at cluster level). These regions remained to show shape effects after controlling for the effects of action kinematics and configuration of hand (Fig. 5, bottom left, voxel $p < 0.01$, FWE corrected $p < 0.05$ at cluster level). For action kinematics, significant correlations were identified in the bilateral MFG, IFG, supplementary motor area and precentral cortex (Fig. 5, top middle, voxel $p < 0.01$, FWE corrected $p < 0.05$ at cluster level). After controlling for object shape and configuration of hand, very similar regions remained significant and extended to the left anterior insula (Fig. 5, bottom middle, voxel $p < 0.01$, FWE corrected $p < 0.05$ at cluster level). Extensive regions of the left LOTC, bilateral posterior occipital cortex, bilateral calcarine and lingual gyrus, bilateral SMG, SPL and postcentral cortex and the bilateral precentral cortex showed significant correlation with RSM of configuration of hand (Fig. 5, top right, voxel $p < 0.01$, FWE corrected $p < 0.05$ at cluster level). After controlling for object shape and action kinematics, none survived the whole-brain multiple comparison corrections under this height threshold (Fig. 5, bottom right). Intriguingly, the right lingual gyrus and surrounding striate cortex showed significant unique effect of hand configuration under the threshold of voxel $p < 0.001$, cluster-level FWE $p < 0.05$. Largely similar patterns were observed for results based on data without demeaning (Supplementary Fig. 2) though the strength of effects slightly differed.

4. Discussion

In the current study, we tried to tease apart the shape and tool-use action using four tools for which these two dimensions were largely orthogonal. Information-based analyses revealed that within the tool network, the bilateral LOTC showed robust effects of shape but could not effectively distinguish between different object-directed actions; the left inferior frontal and precentral regions showed robust action effects; the left parietal region exhibited coding of both shape and action information. The RSA-based analyses, which allows for further tests of shape and finer action components based on post-hoc subjective ratings, confirmed the robust, unique representation of object shapes in the bilateral LOTC and action kinematic components in the left middle/inferior frontal and precentral regions. Beyond the tool-selective network, information-based and RSA-based whole-brain analyses consistently identified the lingual gyrus in coding of both shape and action information. Below we discuss our current findings in each of these regions.

4.1. The representation of object shapes in LOTC and its relation with object-directed actions

When disentangling shape from tool-use action information in the way that we do – i.e., selecting the rare cases where these two dimensions are fully dissociated – the tool-use action would have to be those can only be retrieved from memory instead of being computed

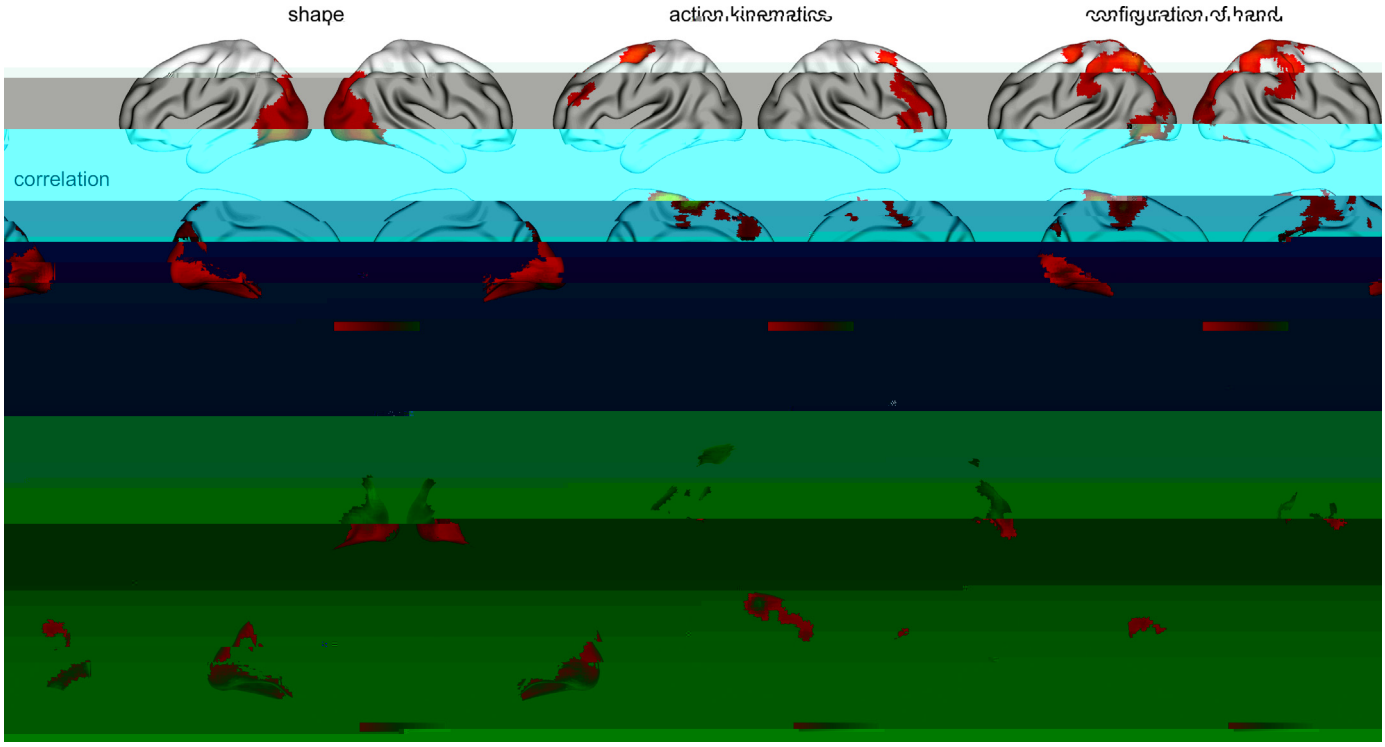

Fig. 5. Results of the whole-brain RSA searchlight. All maps were thresholded at FWE-corrected $p < 0.05$ at the cluster level, with the height threshold of $p < 0.01$, except that the bottom right map of the partial RSA result of the configuration of hand was thresholded at uncorrected $p < 0.01, k > 100$ voxels. Color bars denote t values.

from the object shape. In this case, we observed strong shape representation in the tool-selective LOTC and adjacent regions. This is consistent with the previous literature indicating LOTC's involvement in object shape representation (Peelen and Caramazza, 2012; Fabbri et al., 2016; Bracci et al., 2017; Chen et al., 2017a), and further indicate that the shape effects were independent from tool-use actions in LOTC. Objects are strongly represented in the LOTC according to their shapes (elongated objects together; T-shape objects together) regardless of the actions when people using them.

Although we found extensive regions of the visual cortex that could distinguish between T-shaped vs. I-shaped tools, tool-selective responses (contrasting tools with other objects) were observed in the LOTC but not in other (earlier) visual areas. While most visual areas are sensitive to (domain general) shape distinctions, it is likely that LOTC is more sensitive to certain ones that are associated with those related with tools. In addition, previous studies have found that in comparison to other ventral visual regions the LOTC was functionally connected with frontoparietal visuomotor areas frequently involved in action-related processing (Peelen et al., 2013; Hutchison et al., 2014; Hutchison and Gallivan, 2016; Chen et al., 2017a). The specific connectional profile may make this region an optimal relay station for transforming object shape information to dorsal motor-related regions for action planning (Mahon and Caramazza, 2011; Chen et al., 2017a). Interestingly, among the finer action components we tested, though we did not observe action kinematic representation in LOTC, we did observe significant correlation with hand configuration in this region before controlling for object shapes and action kinematics. It is possible that LOTC cares about shape and the shape-motor mapping (e.g., hand postures) of objects but not about other types of action knowledge that could not be computed from the object shapes. In line with this possibility, a series of studies have reported that LOTC encodes information about the hand-tool relationship (Bracci et al., 2012; Bracci and Peelen, 2013; Buxbaum et al., 2014) and grasping-related properties such as elongation of object shape, grasping axis or number of digits used during grasping (Monaco et al., 2014; Fabbri et al., 2016), indicating LOTC's involvement in representing object-hand interactions.

However, a large body of neuropsychological and neuroimaging studies have reported LOTC's involvement in action representation (Tranel et al., 2003; Kalénine et al., 2010; Watson et al., 2013; Tarhan et al., 2015; Wurm and Lingnau, 2015; Wurm et al., 2017; Bracci et al., 2017; Chen et al., 2017c; see Lingnau and Downing, 2015 for a review). Although in some of these studies the action representation might be correlated with object shapes (Chen et al., 2016, 2017b), most of these findings could not be simply accounted by the shape confound. However, these studies always used video or picture stimuli rich of explicit action information or used tasks requiring explicit retrieval of action information. Therefore, it is possible that the action effects in LOTC would only emerge when action information is apparent or is purposefully retrieved according to task demand. In our current study, we used tool picture stimuli which do not contain explicit action information and adopted a word-picture verification task which does not necessarily engage action retrieval. It is thus possible that experiments with an explicit action task and/or with stimuli directly conveying action information could better reveal the action representations in the LOTC (but see Bracci et al., 2017). Moreover, to achieve our primary goal of strongly disentangle shape and action we have a very limited stimuli space and could only found 4 particular tools, the dissociation between different action components could not be simultaneously optimized (e.g., the high correlation between manners of motion and magnitude of arm movement). Future studies using larger set of tools could be conducted to test the generalizability of our findings and better reveal how different action components related with shape and how they were represented in the tool network.

4.2. Shape and action representations in the parietal cortex

The inferior and superior parietal lobe have been considered as part of the dorsal visual system, which has classically been implicated in

visuomotor control rather than object shape and identity representations (Goodale et al., 1992; Milner and Goodale, 2006; Freud et al.,

References

Bi, Y., Han, Z., Zhong, S., Ma, Y., Gong, G., Huang, R., Song, L., Fang, Y., He, Y., Caramazza, A., 2015. The white matter structural network underlying human tool use and tool understanding. J. Neurosci. 35, 6822–6835. http://dx.doi.org/10.1523/JNEUROSCI.3709-14.2015.

Bi, Y., Wang, X., Caramazza, A., 2016. Object domain and modality in the ventral visual pathway. Trends Cogn. Sci. 20, 282–290. 〈http://linkinghub.elsevier.com/retrieve/pii/S1364661316000437〉.

Bracci, S., Cavina-Pratesi, C., Ietswaart, M., Caramazza, A., Peelen, M.V., 2012. Closely overlapping responses to tools and hands in left lateral occipitotemporal cortex. J. Neurophysiol. 107, 1443–1456. 〈http://jn.physiology.org/content/early/2011/11/23/jn.00619.2011.abstract〉 (Accessed 9 February 2016).

Bracci, S., Daniels, N., Op De Beeck, H., 2017. Task context overrules object-and category-related representational content in the human parietal cortex. Cereb. Cortex 1–12.

Bracci, S., Op de Beeck, H., 2016. Dissociations and associations between shape and category representations in the two visual pathways. J. Neurosci. 36, 432–444.

Bracci, S., Peelen, M.V., 2013. Body and object e□ectors: the organization of object representations in high-level visual cortex reflects body-object interactions. J. Neurosci. 33, 18247–18258. 〈http://www.ncbi.nlm.nih.gov/pubmed/24227734〉.

Bub, D.N., Masson, M.E.J., 2006. Gestural knowledge evoked by objects as part of conceptual representations. Aphasiology 20, 1112–1124. 〈http://citeseerx.ist.psu.edu/viewdoc/summary?doi=10.1.1.68.7484〉 (Accessed 9 August 2017).

Buxbaum, L.J., 2017. Learning, remembering, and predicting how to use tools: distributed neurocognitive mechanisms: comment on Osiurak and Badets (2016). Psychol. Rev. 124, 346–360. http://dx.doi.org/10.1037/rev0000051.

Buxbaum, L.J., Kalenine, S., 2010. Action knowledge, visuomotor activation, and embodiment in the two action systems. Ann. N. Y. Acad. Sci. 1191, 201–218.

Buxbaum, L.J., Kyle, K., Grossman, M., Coslett, H.B., 2007. Special issue: original article left inferior parietal representations for skilled hand-object interactions: evidence from stroke and corticobasal degeneration. Cortex 43, 411–423.

Buxbaum, L.J., Kyle, K.M., Menon, R., 2005. On beyond mirror neurons: internal representations subserving imitation and recognition of skilled object-related actions in humans. Cogn. Brain Res. 25, 226–239. 〈http://linkinghub.elsevier.com/retrieve/pii/S0926641005001643〉 (Accessed 11 July 2017).

Buxbaum, L.J., Sa□ran, E.M., 2002. Knowledge of object manipulation and object function: dissociations in apraxic and nonapraxic subjects. Brain Lang. 82, 179–199.

Buxbaum, L.J., Shapiro, A.D., Coslett, H.B., 2014. Critical brain regions for tool-related and imitative actions: a componential analysis. Brain 137, 1971–1985.

Buxbaum, L.J., Veramontil, T., Schwartz, M.F., 2000. Function and manipulation tool knowledge in apraxia: knowing “what for” but not “how.”. Neurocase 6, 83–97.

Caramazza, A., Hillis, A.E., Rapp, B.C., Romani, C., 1990. The multiple semantics hypothesis: multiple confusions? Cogn. Neuropsychol. 7, 161–189. 〈http://www.tandfonline.com/doi/abs/10.1080/02643299008253441〉 (Accessed 9 August 2017).

Chao, L.L., Haxby, J.V., Martin, A., 1999. Attribute-based neural substrates in temporal cortex for perceiving and knowing about objects. Nat. Neurosci. 2, 913–919.

Chao, L.L., Martin, A., 2000. Representation of manipulable man-made objects in the dorsal stream. Neuroimage 12, 478–484. 〈http://linkinghub.elsevier.com/retrieve/pii/S1053811900906359〉 (Accessed 9 August 2017).

Chen, J., Snow, J.C., Culham, J.C., Goodale, M.A., 2017a. What role does “elongation” play in “tool-specific” activation and connectivity in the dorsal and ventral visual streams? Cereb. Cortex 1–15. 〈https://academic.oup.com/cercor/article-lookup/doi/10.1093/cercor/bhx017〉.

Chen, Q., Garcea, F.E., Jacobs, R.A., Mahon, B.Z., 2017b. Abstract representations of object-directed action in the left inferior parietal lobule. Cereb. Cortex 1–13. Available at. 〈https://www.ncbi.nlm.nih.gov/pubmed/28605410〉.

Chen, Q., Garcea, F.E., Mahon, B.Z., 2016. The representation of object-directed action and function knowledge in the human brain. Cereb. Cortex 26, 1609–1618.

Clarke, S., Miklossy, J., 1990. Occipital cortex in man: organization of callosal connections, related myelo- and cytoarchitecture, and putative boundaries of functional visual areas. J. Comp. Neurol. 298, 188–214. 〈http://doi.wiley.com/10.1002/cne.902980205〉 (Accessed 29 April 2018).

Epstein, R., 2005. The cortical basis of visual scene processing. Vis. Cogn. 12, 954–978. 〈http://www.tandfonline.com/doi/abs/10.1080/13506280444000607〉 (Accessed 12 August 2014).

Epstein, R.A., 2008. Parahippocampal and retrosplenial contributions to human spatial navigation. Trends Cogn. Sci. 12, 388–396. 〈http://www.pubmedcentral.nih.gov/articlerender.fcgi?artid=2858632&tool=pmcentrez&rendertype=abstract〉 (Accessed 9 July 2014).

Epstein, R., Kanwisher, N., 1998. A cortical representation of the local visual environment. Nature 392, 598–601. Available at. 〈http://www.ncbi.nlm.nih.gov/pubmed/9560155〉.

Fabbri, S., Stubbs, K.M., Cusack, R., Culham, J.C., 2016. Disentangling representations of object and grasp properties in the human brain. J. Neurosci. 36, 7648–7662. 〈http://www.ncbi.nlm.nih.gov/pubmed/27445143〉 (Accessed 24 February 2017).

Freud, E., Plaut, D.C., Behrmann, M., 2016. “What” is happening in the dorsal visual pathway. Trends Cogn. Sci. 20, 773–784.

Gallivan, J.P., Chapman, C.S., Mclean, D.A., Flanagan, J.R., Culham, J.C., 2013. Activity patterns in the category-selective occipitotemporal cortex predict upcoming motor actions. Eur. J. Neurosci. 38, 2408–2424.

Garrido, L., Vaziri-Pashkam, M., Nakayama, K., Wilmer, J., 2013. The consequences of subtracting the mean pattern in fMRI multivariate correlation analyses. Front. Neurosci.

Goldenberg, G., 2009. Apraxia and the parietal lobes. Neuropsychologia 47, 1449–1459. 〈http://linkinghub.elsevier.com/retrieve/pii/S0028393208002984〉 (Accessed 14 August 2017).

Goodale, M.A., Milner, A.D., Jakobson, L.S., Carey, D.P., 1991. A neurological dissociation between perceiving objects and grasping them. Nature 349, 154–156.

Goodale, M.A., Milner, A.D., Prablanc, C., Chitty, A.J., Sakata, H., 1992. Separate visual pathways for perception and action. Trends Neurosci. 15, 20–25. 〈http://www.ncbi.nlm.nih.gov/pubmed/1374953〉 (Accessed 14 August 2017).

Grill-Spector, K., Weiner, K.S., 2014. The functional architecture of the ventral temporal cortex and its role in categorization. Nat. Rev. Neurosci. 15, 536–548. Available at. 〈http://www.nature.com/doifinder/10.1038/nrn3747〉.

Haushofer, J., Livingstone, M.S., Kanwisher, N., 2008. Multivariate patterns in object-selective cortex dissociate perceptual and physical shape similarity. PLoS Biol. 6, e187. 〈http://www.pubmedcentral.nih.gov/articlerender.fcgi?artid=2486311&tool=pmcentrez&rendertype=abstract〉 (Accessed 5 August 2014).

Haxby, J., Ho□man, E., Gobbini, M., 2000. The distributed human neural system for face perception. Trends Cogn. Sci. 4, 223–233. Available at. 〈http://www.ncbi.nlm.nih.gov/pubmed/10827445〉.

He, C., Peelen, M.V., Han, Z., Lin, N., Caramazza, A., Bi, Y., 2013. Selectivity for large nonmanipulable objects in scene-selective visual cortex does not require visual experience. Neuroimage 79, 10823.12,-316.9 (2014.)-309.5 (T-s116.1 (Aug36.7 (n-3689435.5 (5_uir

2014).
Martin, A., Wiggs, C.L., Ungerleider, L.G., Haxby, J.V., 1996. Neural correlates of category-specific knowledge. Nature 379, 649–652. Available at. 〈http://www.nature.com/doifinder/10.1038/379649a0%5Cnhttp://www.ncbi.nlm.nih.gov/sites/entrez?Db=pubmed&DbFrom=pubmed&Cmd=Link&LinkName=pubmed_pubmed&LinkReadableName=RelatedArticles&IdsFromResult=8628399&ordinalpos=3&itool=EntrezSystem2.PEntrez.Pubmed.Pu〉.
Milner, A.D., Goodale, M.A., 2006. The Visual Brain in Action. Oxford University Press.
Monaco, S., Chen, Y., Medendorp, W.P., Crawford, J.D., Fiehler, K., Henriques, D.Y.P., 2014. Functional magnetic resonance imaging adaptation reveals the cortical networks for processing grasp-relevant object properties. Cereb. Cortex 24, 1540–1554.
Mruczek, R.E.B., Loga, I.S. Von, Kastner, S., 2013. The representation of tool and non-tool object information in the human intraparietal sulcus. J. Neurophysiol. 109, 2883–2896.
Negri, G.A.L., Rumiati, R.I., Zadini, A., Ukmar, M., Mahon, B.Z., Caramazza, A., 2007. What is the role of motor simulation in action and object recognition? Evidence from apraxia. Cogn. Neuropsychol. 24, 795–816.
Noppeney, U., Price, C.J., Penny, W.D., Friston, K.J., 2006. Two distinct neural mechanisms for category-selective responses. Cereb. Cortex 16, 437–445.
Oldfield, R.C., 1971. The assessment and analysis of handedness: the Edinburgh inventory. Neuropsychologia 9, 97–113. 〈http://linkinghub.elsevier.com/retrieve/pii/0028393271900674〉 (Accessed 9 August 2017).
Op de Beeck, H.P., 2010. Against hyperacuity in brain reading: spatial smoothing does not hurt multivariate fMRI analyses? Neuroimage 49, 1943–1948.
Peelen, M.V., Bracci, S., Lu, X., He, C., Caramazza, A., Bi, Y., 2013. Tool Selectivity in Left Occipitotemporal Cortex Develops without Vision. :1225–1234.
Peelen, M.V., Caramazza, A., 2012. Conceptual object representations in human anterior temporal cortex. J. Neurosci. 32, 15728–15736. Available at. 〈http://www.ncbi.nlm.nih.gov/pubmed/23136412〉.
Peelen, M.V., Downing, P.E., 2005. Selectivity for the human body in the fusiform gyrus. J. Neurophysiol. 93, 603–608. 〈http://www.ncbi.nlm.nih.gov/pubmed/15295012〉 (Accessed 1 August 2014).
Peelen, M.V., He, C., Han, Z., Caramazza, A., Bi, Y., 2014. Nonvisual and visual object shape representations in occipitotemporal cortex: evidence from congenitally blind and sighted adults. J. Neurosci. 34, 163–170. Available at. 〈http://www.ncbi.nlm.nih.gov/pubmed/24381278〉.
Proklova, D., Kaiser, D., Peelen, M.V., 2016. Disentangling representations of object shape and object category in human visual cortex: the animate–inanimate distinction. J. Cogn. Neurosci. 28, 680–692. 〈http://www.mitpressjournals.org/doi/10.1162/jocn_a_00924〉 (Accessed 1 March 2017).
Riddoch, M.J., Humphreys, G.W., Coltheart, M., Funnell, E., 1988. Semantic systems or system? Neuropsychological evidence re-examined. Cogn. Neuropsychol. 5, 3–25. 〈http://www.tandfonline.com/doi/abs/10.1080/02643298808252925〉 (Accessed 9 August 2017).
Rizzolatti, G., Cattaneo, L., Fabbri-Destro, M., Rozzi, S., 2014. Cortical mechanisms underlying the organization of goal-directed actions and mirror neuron-based action understanding. Physiol. Rev. 94, 655–706. 〈http://www.ncbi.nlm.nih.gov/pubmed/24692357〉 (Accessed 14 August 2017).
Rizzolatti, G., Craighero, L., 2004. The mirror-neuron system. Annu. Rev. Neurosci. 27, 169–192. 〈http://www.annualreviews.org/doi/10.1146/annurev.neuro.27.070203.144230〉 (Accessed 14 August 2017).
Rizzolatti, G., Sinigaglia, C., 2010. The functional role of the parieto-frontal mirror circuit: interpretations and misinterpretations. Nat. Rev. Neurosci. 11, 264–274. 〈http://www.nature.com/doifinder/10.1038/nrn2805〉 (Accessed 14 August 2017).
Sayres, R., Grill-Spector, K., 2008. Relating retinotopic and object-selective responses in human lateral occipital cortex. J. Neurophysiol. 100, 249–267. Available at. 〈http://jn.physiology.org/cgi/doi/10.1152/jn.01383.2007〉.
Schwarzlose, R.F., Baker, C.I., Kanwisher, N., 2005. Separate face and body selectivity on the fusiform gyrus. J. Neurosci. 25, 11055–11059. 〈http://www.ncbi.nlm.nih.gov/pubmed/16306418〉 (Accessed 24 July 2014).
Tarhan, L.Y., Watson, C.E., Buxbaum, L.J., 2015. Shared and distinct neuroanatomic regions critical for tool-related action production and recognition: evidence from 131 left-hemisphere stroke patients. J. Cogn. Neurosci. 27, 2491–2511.
Tranel, D., Kemmerer, D., Adolphs, R., Damasio, H., Damasio, A.R., 2003. Neural correlates of conceptual knowledge for actions. Cogn. Neuropsychol. 20, 409–432. (Available at). 〈http://www.tandfonline.com/doi/abs/10.1080/02643290244000248〉.
Tsao, D.Y., Moeller, S., Freiwald, W.A., 2008. Comparing face patch systems in macaques and humans. Proc. Natl. Acad. Sci. USA 105, 19514–19519. Available at. 〈http://www.pubmedcentral.nih.gov/articlerender.fcgi?artid=2614792&tool=pmcentrez&rendertype=abstract〉.
Tzourio-Mazoyer, N., Landeau, B., Papathanassiou, D., Crivello, F., Etard, O., Delcroix, N., Mazoyer, B., Joliot, M., 2002. Automated anatomical labeling of activations in SPM using a macroscopic anatomical parcellation of the MNI MRI single-subject brain. Neuroimage 15, 273–289.
Vannuscorps, G., Andres, M., Pillon, A., 2014. Is motor knowledge part and parcel of the concepts of manipulable artifacts? Clues from a case of upper limb aplasia. Brain Cogn. 84, 132–140. 〈http://linkinghub.elsevier.com/retrieve/pii/S0278262613001723〉 (Accessed 9 August 2017).
Warrington, E.K., McCarthy, R.A., 1987. Categories of knowledge. Brain 110, 1273–1296. 〈http://brain.oxfordjournals.org/content/110/5/1273〉 (Accessed 11 November 2015).
Watson, C.E., Buxbaum, L.J., 2014. Journal of experimental psychology: human perception and performance uncovering the architecture of action semantics uncovering the architecture of action semantics. J. Exp. Psychol. Hum. Percept. Perform. http://dx.doi.org/10.1037/a0037449.
Watson, C.E., Buxbaum, L.J., Watson, C.E., Buxbaum, L.J., 2014. Uncovering the architecture of action semantics. J. Exp. Psychol.: Hum. Percept. Perform.
Watson, C.E., Cardillo, E.R., Ianni, G.R., Chatterjee, A., 2013. Action concepts in the brain: an activation likelihood estimation meta-analysis. J. Cogn. Neurosci. 25, 1191–1205. 〈http://www.mitpressjournals.org/doi/10.1162/jocn_a_00401〉 (Accessed 4 July 2017).
Wurm, M.F., Caramazza, A., Lingnau, A., 2017. Action categories in lateral occipitotemporal cortex are organized along sociality and transitivity. J. Neurosci. 37, 562–575.
Wurm, M.F., Lingnau, A., 2015. Decoding actions at di□erent levels of abstraction. J. Neurosci. 35, 7727–7735.
Xia, M., Wang, J., He, Y., 2013. BrainNet Viewer: a network visualization tool for human brain connectomics. PLoS One 8, e68910. 〈http://www.pubmedcentral.nih.gov/articlerender.fcgi?artid=3701683&tool=pmcentrez&rendertype=abstract〉 (Accessed 17 July 2014).
Zachariou, V., Klatzky, R., Behrmann, M., 2014. Ventral and dorsal visual stream contributions to the perception of object shape and object location. J. Cogn. Neurosci. 26, 189–209. 〈http://www.mitpressjournals.org/doi/10.1162/jocn_a_00475〉 (Accessed 9 August 2017).
Zinchenko, E., Snedeker, J., 2011. The Role of Functions and Motor Actions in Early Tool Concepts. Fac Arts Sci Harvard Univ.